Prepared for submission to JCAP

Primordial Power Spectra Reconstruction Constrained by a Measured Tensor Amplitude

J. Richard Bond[a] **Jonathan Braden**[a,b] **Andrei Frolov**[c] **Zhiqi Huang**[a] **Pascal Vaudrevange**[d]

[a]CITA
[b]Dept. of Physics, U of T
[c]Simon Fraser University
[d]Germany

E-mail: bond@cita.utoronto.ca, jbraden@cita.utoronto.ca, frolov@sfu.ca, zqhuang@cita.utoronto.ca

Abstract. The shapes of the primordial scalar power spectra are the key quantities to unravel the physics of the inflationary epoch. Blahblah...

Contents

1 Introduction

The cosmic microwave background radiation is a unique window into the physics of energy scales above TeV. Progress towards harvesting its information content has been steady on the experimental side, starting with the COBE experiment [1], continuing with balloon borne experiments such as Boomerang [2, 3], ground-based experiments such as ACT [4, 5], SPT [6, 7] and BICEP [8], and the satellites WMAP [9, 10] and Planck [11–13]. They delivered a picture of a universe that is extremely homogeneous: Gaussian fluctuations sit on top of a uniform background of photons that stream to us from the surface of last scattering at redshift about 1100, with an amplitude of about 10^{-5}. Decomposing this image of the microwave sky into spherical harmonics shows an angular power spectrum whose features are well understood. Acoustic oscillations in the primordial photon-baryon fluid freeze out at the surface of last scattering, with the photons streaming (almost) freely towards us, showing the familiar acoustic peaks in the angular power spectrum. Their locations and relative amplitudes allow us to infer the energy content of the universe.

While experimental advances have been formidable, the exact properties of microscopic theories responsible for the inflationary period remain elusive. A plethora of different scalar field potentials have been suggested, and many of them are compatible with current observations. From a theoretical perspective, the best that can be said is that there are many scalar fields in string theory. As for their potentials, not much is known. Even though some advances have been made in building models of inflation based on or inspired by string theory [14–20], the vast majority of the string landscape is still unchartered.

Traditionally the inflationary dynamics are described in the slow-roll approximation, assuming that the inflaton field rolls slowly (or with small acceleration) down its potential. For the simplest single-field slow-roll models, both the scalar and tensor power spectra are very close to power-law and the tilt of tensor power spectrum satisfies a consistency-relation. As a consequence, as far as only observables are concerned, these models can be described with three parameters: the amplitude of the scalar power spectrum (A_s), the tilt of the scalar power spectrum ($n_s - 1$), and the tensor-to-scalar ratio ($r \equiv A_T/A_s$ where A_T is the amplitude of tensor power spectrum). The tilt of the tensor power spectrum, according to slow-roll approximation, is $n_t = -r/8$.

Thanks to the plethora of observational data that are already available today, we can go beyond the simplest models and ask whether a single-field slow-roll model is adequate to describe the data. To answer such a question it is necessary to extend the parameter space with reasonable theoretical motivations. For a broad class of models, the tensor power spectrum remains to be a power-law with a small tilt. This is because the tensor power

spectrum, almost model-independently, only depends on the energy scale of inflation, which by definition does not vary much. Observationally, because of the smallness of B-mode polarization signature and the limited range of scales where tensor power spectrum can be measured, it is very difficult to measure features in the tensor power spectrum. Thus, it is reasonable to keep the parametrization of tensor power spectrum unchanged. For the future, we might be able to explore the small tilt of tensor power spectrum and test the sinlg-field slow-roll consistency relation. In that case, n_t should be introduced as a free parameter. For the current data, we do not bother to do so as n_t at this stage is far from being measurable to the accuracy of testing the consistency relation. However, while a broader class of inflation models are permitted, the scalar power spectrum, becomes very model-dependent [21–25]. Phenomenologically, back to the early COBE era, a running parameter $n_{\rm run}$ was already introduced as a minimal extension to describe the scale dependence of the tilt of scalar power spectrum [26]. Theoretically, a tiny running $\lesssim 10^{-3}$ is expected from single-field slow-roll models. A detectable running $\gtrsim 0.01$ requires a very slow phase-transition over many efolds of inflation, which is not very well motivated. However, if only one or two degrees of freedom are to be added, there is no "optimal" or "universal" parameterization that can describe a much broader class of models. For this reason, the running parameter remains to be "the standard extension" to date. This situation, however, can be changed if we add more degrees of freedom into the parametrization. Because the observable range of cosmological scales is about ten efolds, a function interpolated from about 10 knots can cover most of the features that are not much shaper than one efold in scale. This interpolation method, to be thoroughly explored in this paper, provides an alternative approach to study the primordial power spectra with very little theoretical priors imposed. The philosophy here is to let the data guide our theoretical thoughts.

If we only consider the CMB temperature-temperature (TT) auto-correlation, the immediate problem of allowing an "arbitrary" shape of scalar power spectrum is that the tensor contribution to the TT correlation can be mimicked by a scalar power spectrum with a proper shape. There is hence a strong degeneracy between the scalar and tensor power spectra. The theoretical prediction of the amplitude of tensor power spectrum varies from $r \sim 10^{-10}$ for many string-motivated small-field models to $r \sim 0.1$ for large-field models, with the scales in between almost all plausible. Thus, this degeneracy cannot be relieved by imposing a theoretical prior. We need additional data to constrain the tensor power spectrum independently. The recent detection of B-mode polarization in CMB [8], although remains to be confirmed by other experiments, casts a light on solving this problem.

This paper is structured as follows. Blahblah...

2 Reconstructing Primordial Trajectories

Following the convention in the literarture we use $\Delta^2_S(k) \equiv \frac{k^3 P_S(k)}{2\pi^2}$ and $\Delta^2_T(k) \equiv \frac{k^3 P_T(k)}{2\pi^2}$ to denote the scalar- and tensor power spectra, respectively. These power spectra are k-volumed weighed, and are nearly flat for most of the inflation models.

The CMB temperature-temperature angular power spectrum C_ℓ^{TT} from tensor contribution with $r = 0.2$ (the central value suggested by BICEP2 [8]) can be generated by an effective scalar power spectrum shown in Figure 1. To avoid this degeneracy between tensor- and scalar contributions, we can either assume r to be some specific value and discuss the constraints on scalar power spectrum under such an assumption, or use BICEP2 data to independently constrain the tensor power spectrum. We will apply both approaches in this

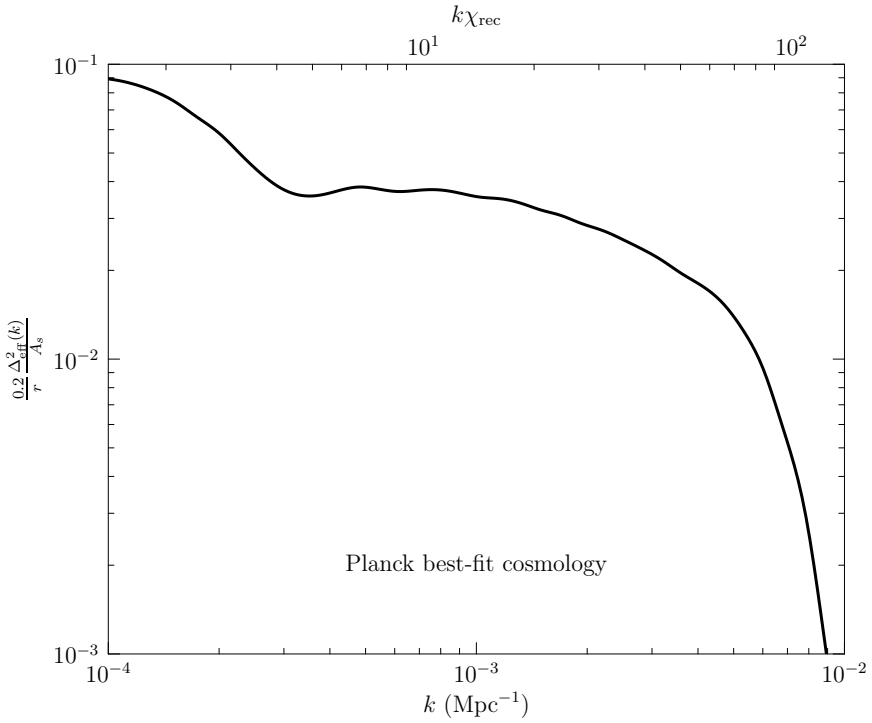

Figure 1. The effective scalar power spectrum that produces the same C_ℓ^{TT} as $r = 0.2$ tensor power spectrum would do. Planck best-fit cosmology is assumed.

section. When fixing r we use fiducial values $r = 0.02$, 0.2 and 0.5 as typical examples, whereas for "free" r we use a flat prior $0 \leq r < 1$. The lower bound $r \geq 0$ is defined by theory, while the assumed upper bound $r < 1$ does not affect the result as long as it is much higher than the observational upper bound, which, from BICEP2 is about 0.4 at 99.7% confidence level.

We use the public available software CosmoMC [27] to do Monte Carlo Markov Chain (MCMC) calculations. The software is modified to include our parametrization of the primordial power spectra. For the runs with fixed r, we use Planck data including lensing (Planck), WMAP polarization (WP), ACT and SPT high-ell data (highL) and Baryon Acoustic Oscillations (BAO) constraint from Sloan Digital Sky Survey (SDSS) [28] and Six-degree-Field Galaxy Survey (6dF) [29, 30]. The BICEP2 data is used only for runs with r varying. We use 11 knots as a representative case. We verify, by varying the number of knots (typically, from 9 to 15), that the results are not sensitive to the number of knots.

A n-knots parametrization is constructed by interpolating scalar power spectrum between n knots. In our parametrization, A_s is still defined as the amplitude of scalar power sepctrum at $k_{\rm pivot} = 0.05{\rm Mpc}^{-1}$. The knots k_1, k_2, ..., k_n are uniform in $\ln k$, with $k_{\rm pivot}$ being one of the knots $k_{i_p} = k_{\rm pivot}$ (i_p is a fixed integer between 1 and n). Additional $n-1$ parameters are introduced to describe the deviation from scale-invariance. They are defined as $\gamma_i \equiv \Delta^2_S(k_i)/A_s$, for $i = 1, 2, \ldots, i_p - 1, i_p + 1, \ldots, n$. The choice of i_p and spacing $\delta \ln k \equiv \ln(k_{i+1}/k_i)$ depends on the number of knots. The criterion is that the relevant cosmological scales (roughly from $10^{-4}{\rm Mpc}^{-1}$ to $0.2{\rm Mpc}^{-1}$) are covered from k_1 to k_n. For the MCMC runs we assume flat prior on $\ln A_s$ and $\ln \gamma_i$ ($i \neq i_p$). For scales between k_1 and k_n,

we cubic-spline interpolate $\ln(\Delta_S^2(k)/A_s)$ with natural boundary conditions (second derivatives vanish). Whereas for scales beyond, we simply assume $\Delta_S^2(k) = \Delta_S^2(k_1)$ for $k < k_1$ and $\Delta_S^2(k) = \Delta_S^2(k_n)$ for $k > k_n$. As for the tensor power spectrum, we use a parametrization $\Delta_T^2(k) = rA_s(k/k_{\rm pivot})^{n_t}$ with $n_t = -r/8$ enforced. Note that in the literature r is often defined as the tensor-to-scalar ratio at $k = 0.002{\rm Mpc}^{-1}$, slightly different from the r defined here. We do not adopt this convention because with our parametrization, the scalar power at $k = 0.002{\rm Mpc}^{-1}$ is poorly measured, whereas the conventional parametrization extrapolates the scalar power to all scales with a constant n_s. In all the runs we use a prior $-2 \leq \ln\gamma_i \leq 2$ $(i = 1, 2, \ldots, i_p - 1, i_p + 1, \ldots, n)$. For most of the knots this prior does not matter, as the data only allow a much narrower range of $\ln\gamma_i$. However, for the superhorizon scales $k \lesssim 10^{-4}{\rm Mpc}^{-1}$ and very small scales $k \gtrsim 0.2{\rm Mpc}^{-1}$ that are not measured by the cosmological data, the prior will dominate the results.

In Fig 2 we show the reconstructed scalar power spectrum under different assumptions about r. In the prior dominated scales ($k \leq 10^{-4}{\rm Mpc}^{-1}$ and $k \gtrsim 0.2{\rm Mpc}^{-1}$), the trajectories tend to uniformly scan the allowed prior $-2 \leq \ln\gamma_i \leq 2$. In the observable-scale range, however, the trajectories tend to bend down (w.r.t. power-law extrapolation) at $10^{-4}{\rm Mpc}^{-1} \lesssim k \lesssim 0.01{\rm Mpc}^{-1}$. This tendency is more significant for larger r (either put in by hand or constrained by BICEP2), because a deficit in scalar power at $k \lesssim 0.01{\rm Mpc}^{-1}$ is needed to cancel the tensor contribution to C_ℓ^{TT}. As shown in Fig 3, although the reconstructed scalar power spectra differ significantly between large and small r's cases, the C_ℓ^{TT} trajectories remain similar.

The scalar power deficit on large scales does not necessarily come with a simple shape. The spectrum can bend all the way down to superhorizon scales, or have one or two dips. The data on large scales do not have sufficient statistical power to measure the detailed shape. The power deficit in $\Delta_s^2(k)$ is caused by an observed low-ℓ power deficit in Planck temperature C_ℓ data. We discuss this in Section 3.

3 The low-ℓ Power Deficit

Planck reported a tension between the Planck best-fit ΛCDM model and the low-ℓ spectrum in the form of a power deficit of 5-10% at $l \lesssim 40$, with a statistical significance of 2.5-3σ [12]. The Planck analysis used a modified Hausman test, where the lower-bound $\ell_{\rm min}$ is fixed to be 2 and the contributions from the proximy of upper-bound $\ell_{\rm max}$ are filtered by a smoothly damping window. Thus, the exact ℓ range contributing to the anomaly has not been identified in details. Here we use a different and more intuitive way to identify the anomaly ℓ-range.

In Fig 4 Planck C_ℓ^{TT} data are plotted against the best-fit ΛCDM (without BICEP2 constraint) and ΛCMD + r (with BICEP2 constraint) models to demonstrate the low-ℓ power deficit anomaly. A coherent power deficit between $\ell = 20$ and $\ell = 30$ can be easily identified by eye. The C_ℓ data are not perfectly uncorrelated at low-ℓ, making the understanding of the anomaly sophisticated. However, we can assume a full-sky cosmic-variance limited experiment for an order-of-magnitude estimation. Once an analytic understanding of the anomaly is achieved, we proceed with a more exact MCMC calculation.

We can approximately consider the observed C_ℓ above or below the model predicted ensemble average as a random binary event for each ℓ. The probability of seeing m cotinuous identical bits in a sequence of n random bits, $P(m, n)$, can be computed using $P(m, 0) = P(m, 1) = P(m, 2) = \ldots = P(m, m-1) = 0$, $P(m, m) = 1/2^{m-1}$ and the recurrence relation $P(m, n+1) = P(m, n) + (1 - P(m, n-m))/2^m$ $(n \geq m)$. If we take about 100

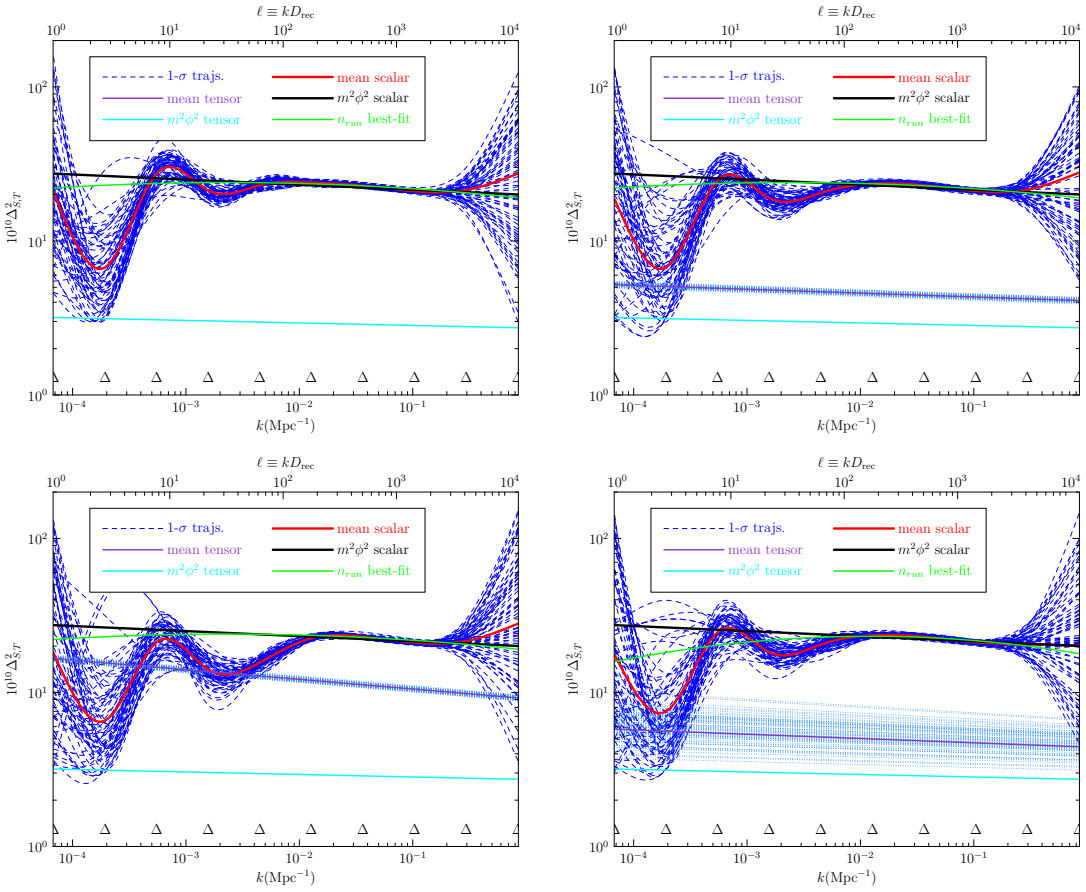

Figure 2. The reconstructed power spectrum with $r = 0.02$, $r = 0.2$, $r = 0.5$ and free r for top-left, top-right, bottom-left, bottom-right panels, respectively. The location of 11 knots used for interpolation are marked with Δ symbols. Data: Planck + highL + BAO. BICEP2 data is added in the free r case.

multipoles as "low-ℓ", the probability of seeing the $20 \leq \ell \leq 30$ power deficit is then about $P(11, 100) \approx 4\%$. So far we have not taken into account the amplitude of the power deficit. Assuming a coherent power deficit is already seen, the probability of seeing a weighed mean power deficit that is at least as large as the observed one, approximated using the central limit theorem, is

$$P = \frac{1}{2}\mathrm{Erfc}\left[\frac{\sum_{\ell=\ell_{\rm min},\ell_{\rm max}}(2\ell+1)\left(1-\sqrt{\frac{4}{\pi(2\ell+1)}}-\frac{C_\ell^{\rm data}}{C_\ell^{\rm model}}\right)}{2\sqrt{\left(1-\frac{2}{\pi}\right)(\ell_{\rm max}-\ell_{\rm min}+1)(\ell_{\rm max}+\ell_{\rm min}+1)}}\right] . \tag{3.1}$$

Here $C_\ell^{\rm data}$ is the planck temperature power spectrum and $C_\ell^{\rm model}$ is computed for a theoretical model. For the anomaly we are interested in ($\ell_{\rm min} = 20$ and $\ell_{\rm max} = 30$), the results are P = 55% for the best-fit ΛCDM model (without BICEP2 constraint) and P = 31% for the best-fit ΛCDM + r model (with BICEP2 constraint). Combining the above discussions, we conclude that the $20 \leq \ell \leq 30$ power deficit is a $\sim 2\%$ rare event for Planck best-fit ΛCDM model, and a $\sim 1\%$ rare event for Planck + BICEP2 best-fit ΛCDM + r model.

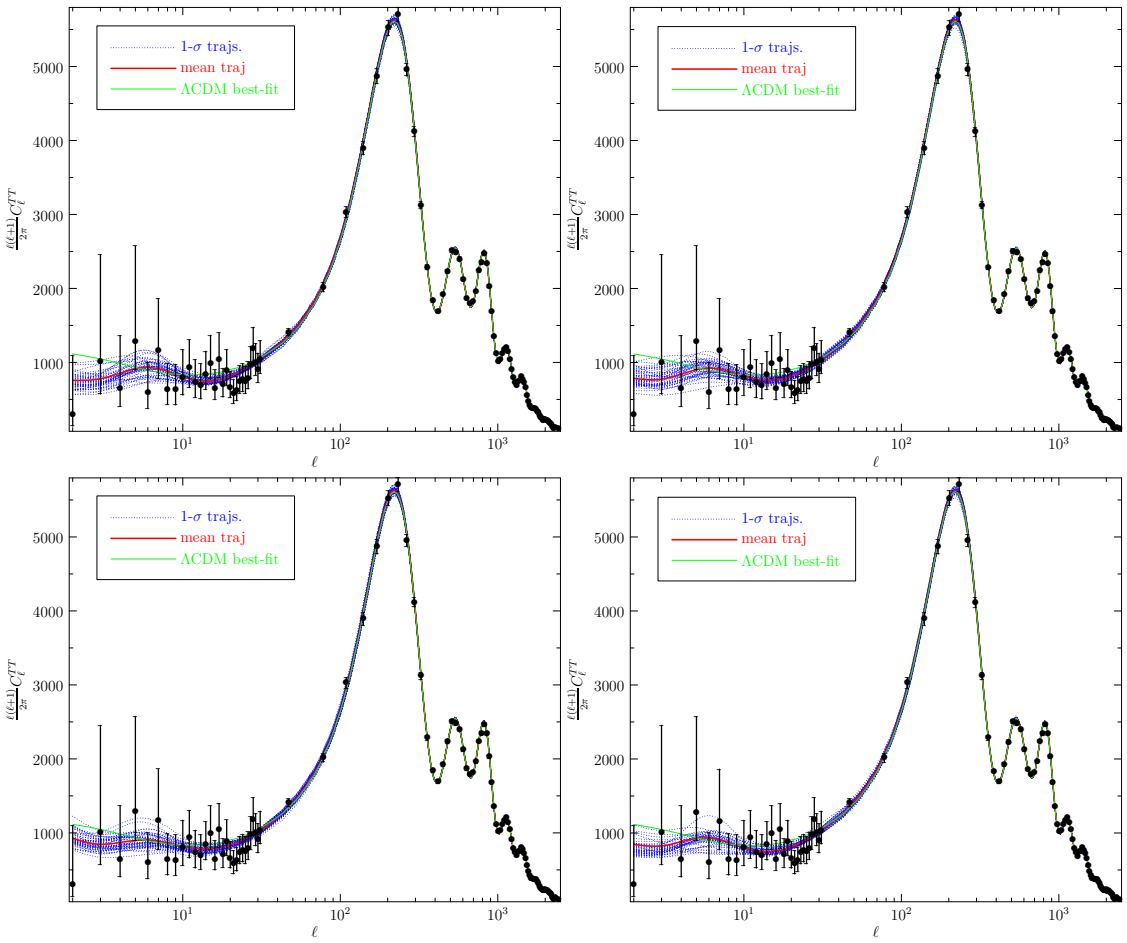

Figure 3. The reconstructed CMB temperature power spectrum with $r = 0.02$, $r = 0.2$, $r = 0.5$ and free r for top-left, top-right, bottom-left, bottom-right panels, respectively. Data: Planck + highL + BAO. BICEP2 data is added in the free r case.

In practice the low-ℓ data are correlated and the above estimation may not be accurate. To study the anomaly more rigorously, we use a "dip parameter" $A_{\rm dip}$ to phenomenologically describe a power deficit between $\ell_{\rm min}$ and $\ell_{\rm max}$. We take the model to be ΛCDM + r + $n_{\rm run}$ so that we can see whether a running or a power deficit is more preferred by the data. The input C_ℓ in the likelihood code is $C_\ell^{\rm model}e^{-A_{\rm dip}}$ if $\ell_{\rm min} \leq \ell \leq \ell_{\rm max}$ and $C_\ell^{\rm model}$ otherwise. We have tried various ℓ ranges. A full list of the ℓ ranges and the corresponding marginalized constraints on $n_{\rm run}$ and $A_{\rm dip}$ are listed in Table 1. A power deficit is favored by the data for $20 \leq \ell \leq 30$ at 3-σ level and for $2 \leq \ell \leq 30$ at 2.7-σ level. We see that in the very-low-ℓ range ($2 \leq \ell \leq 19$ or even lower $2 \leq \ell \leq 8$) the data do not really favor a coherent deficit against a running, whereas for $20 \leq \ell \leq 30$ the data do. This is consistent with Fig 4. The very-low-ℓ data on average, however, are still lower than the ΛCDM prediction. Including the very-low ℓ's for the power deficit does help to relax $n_{\rm run}$ toward zero. To demonstrate the degeneracy between $n_{\rm run}$ and $A_{\rm dip}$ for various choices of $\ell_{\rm min}$ and $\ell_{\rm max}$, we show the 1-σ and 2-σ constraints in the $n_{\rm run}$-$A_{\rm dip}$ space in Fig 5.

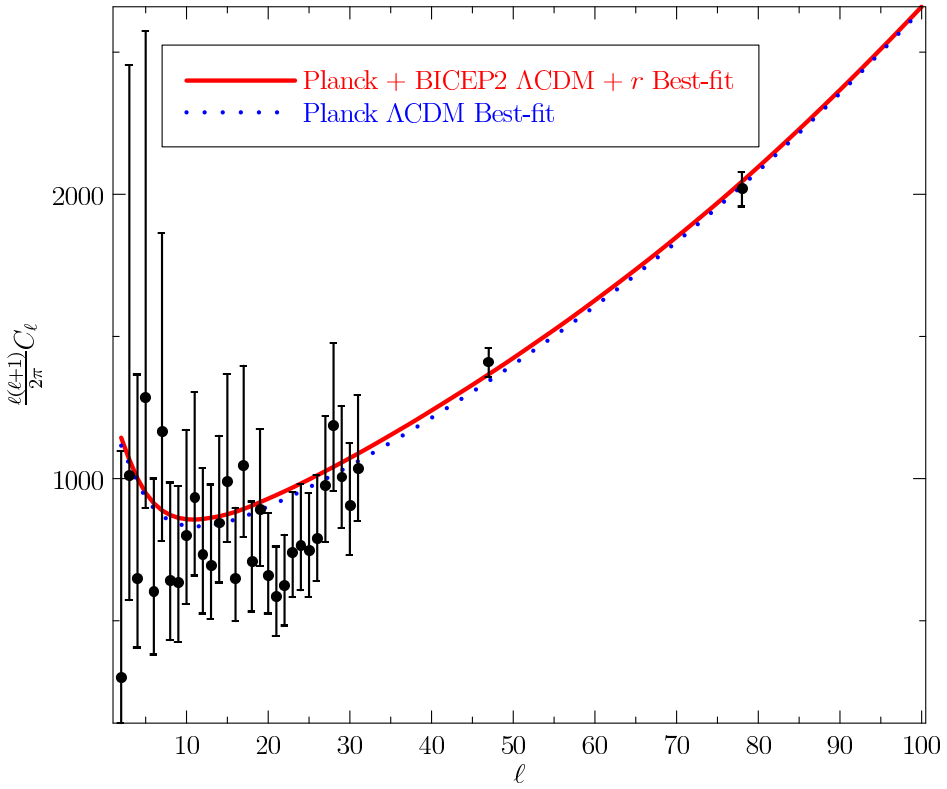

Figure 4. The Planck C_ℓ^{TT} data (binned for $\ell \geq 32$) compared to predictions from best-fit models.

Table 1. Margiinalized 95.4% CL constraints on $n_{\rm run}$ and $A_{\rm dip}$

$\ell_{\rm min}$	$\ell_{\rm max}$	$n_{\rm run}$	$A_{\rm dip}$	significance of $A_{\rm dip} > 0$
none	none	$-0.028^{+0.016}_{-0.017}$	none	none
20	30	$-0.020^{+0.016}_{-0.018}$	$0.18^{+0.12}_{-0.11}$	3σ
2	8	$-0.030^{+0.017}_{-0.018}$	$-0.08^{+0.25}_{-0.27}$	none
2	19	$-0.030^{+0.019}_{-0.020}$	$-0.02^{+0.15}_{-0.15}$	none
2	30	$-0.011^{+0.020}_{-0.020}$	$0.16^{+0.12}_{-0.12}$	2.7σ
2	40	$-0.023^{+0.021}_{-0.022}$	$0.04^{+0.10}_{-0.10}$	none
31	50	$-0.031^{+0.016}_{-0.017}$	$-0.049^{+0.084}_{-0.085}$	none
51	80	$-0.021^{+0.018}_{-0.021}$	$0.053^{+0.070}_{-0.067}$	none

4 Implications for Single-field Inflation Models

Assuming the underlying physics is single-field inflation, we can reverse-engineer the scalar and tensor power spectra to obtain the expansion history $\epsilon \equiv -\dot{H}/H^2$ and the inflaton potential $V(\phi)$. To the lowest order, the reconstruction is

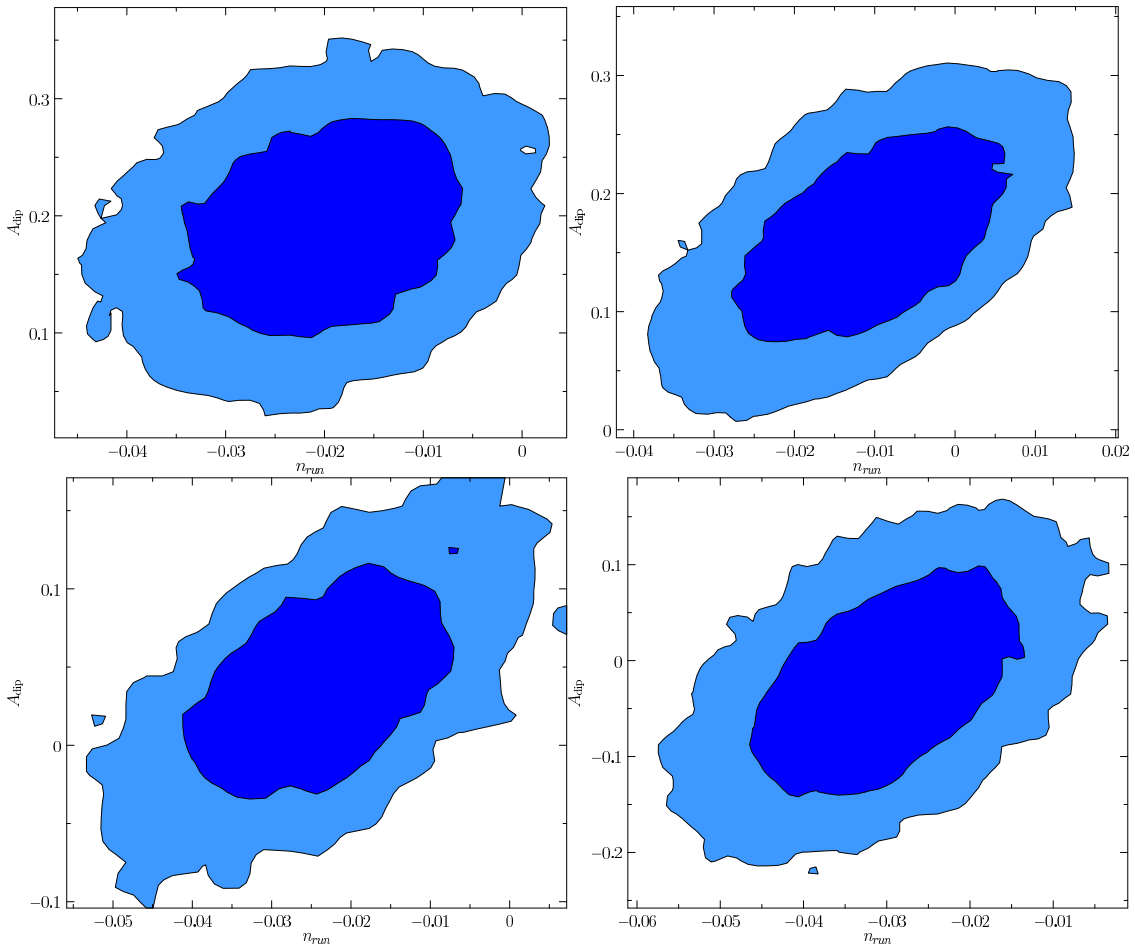

Figure 5. The 68.3% CL and 95.4% CL constraints on $n_{\rm run}$ and $A_{\rm dip}$ for the phenomenological power deficit model. The ℓ ranges are: top-left panel 20-30; top-right panel 2-30; lower-left panel 2-40; lower-right panel 2-19. Data sets: Planck + highL + BICEP2 + BAO.

$$\epsilon(k) \approx \frac{\Delta_T^2(k)}{16\Delta_S^2(k)}\,, \tag{4.1}$$

$$\phi(k) \approx \phi_{\rm pivot} \pm M_p \int_{k_{\rm pivot}}^{k} \sqrt{2\epsilon(k')}\frac{dk'}{k'}\,, \tag{4.2}$$

$$V(k) \approx V_{\rm pivot} e^{\int_{k_{\rm pivot}}^{k} 2\epsilon(k')\frac{dk'}{k'}}\,, \tag{4.3}$$

where $\phi_{\rm pivot}$ and $V_{\rm pivot}$ are the field and potential values when the pivot mode $k_{\rm pivot} = 0.05{\rm Mpc}^{-1}$ exits the horizon. The choice of $\phi_{\rm pivot}$ and $\pm$ in eq. (4.2) is arbitrary and is just a matter of redefining the field. We use + sign convention so that larger ϕ corresponds to larger wavenumber k and smaller scales. The pivot potential $V_{\rm pivot}$ can be determined using

$$V_{\rm pivot} \approx \frac{(3-\epsilon(k_{\rm pivot}))\,M_p^4}{16}\Delta_T^2(k_{\rm pivot})\,. \tag{4.4}$$

We show the reconstructed ϵ and $\ln V/V_{\rm pivot}$ trajectories in Fig 6 and Fig 7. The reconstructions are done using 11 knots. For various cases we have verified that the reconstruction

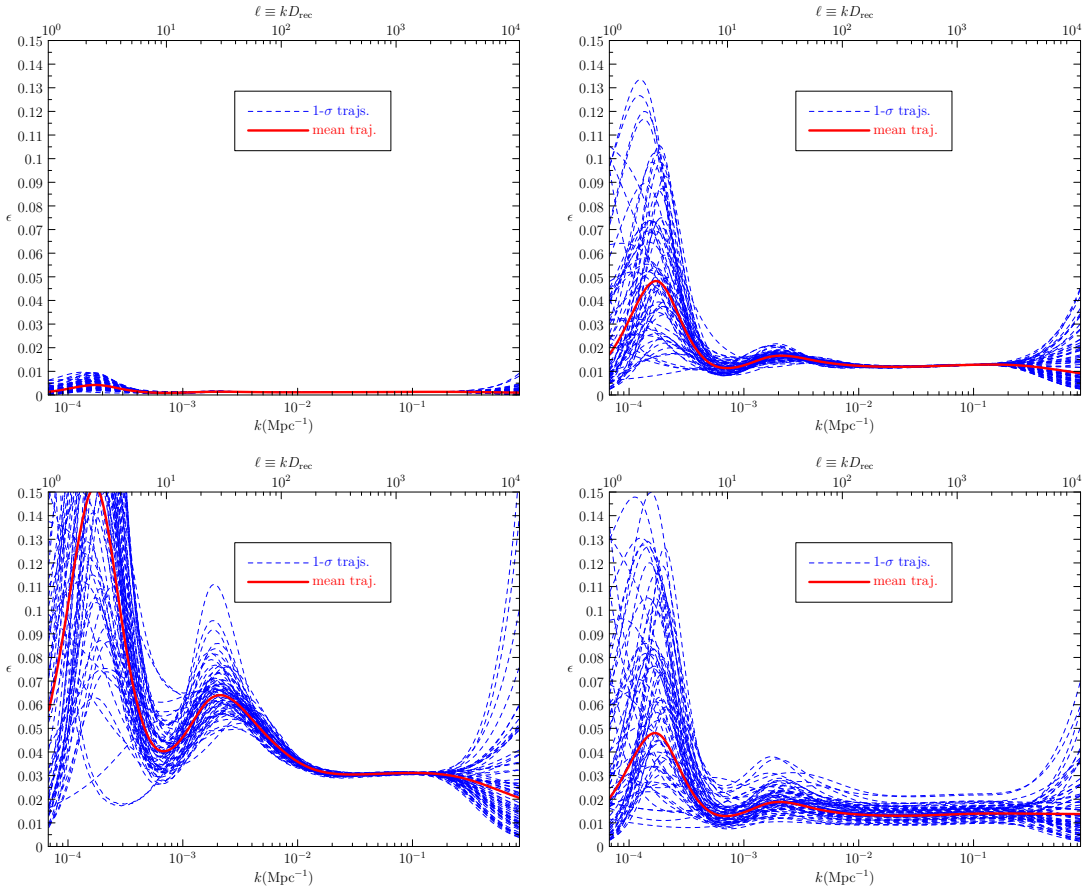

Figure 6. The reconstructed ϵ trajectories with $r = 0.02$, $r = 0.2$, $r = 0.5$ and free r for top-left, top-right, bottom-left, bottom-right panels, respectively. Data: Planck + highL + BAO. BICEP2 data is added in the free r case.

is not senstive to the number of knots by varying the number of knots from 9 to 15. The potential trajectories tend to bend up on large scales (negative $\phi - \phi_{\rm pivot}$). This is caused by the large-scale power deficit discussed in previous sections.

After all, the purpose of doing the "model-independent" reconstruction is to obtain an idea what kind of models the data are driving us towards. The large-scale power deficit drives us to search for a model that allows deviations from power-law scalar power spectrum, where the deviatioins should be

1. strongly suppressed on small scales;

2. allowing various shapes: simple bending-down, one or two dips, damping oscillations, etc.

We propose a simple single-field model with potential

$$V(\phi) = \frac{1}{2}m^2\phi^2\left[1 + \frac{\mu}{2}(1 + \tanh\frac{\phi - \phi_c}{\delta\phi})\right] . \tag{4.5}$$

To map the potential to the scalar and tensor power spectra, we need five parameters: m, μ, ϕ_c, $\delta\phi$ and $N_{\rm inf}$, the number of efolds from the time when $k_{\rm pivot}$ exits the horizon to the end

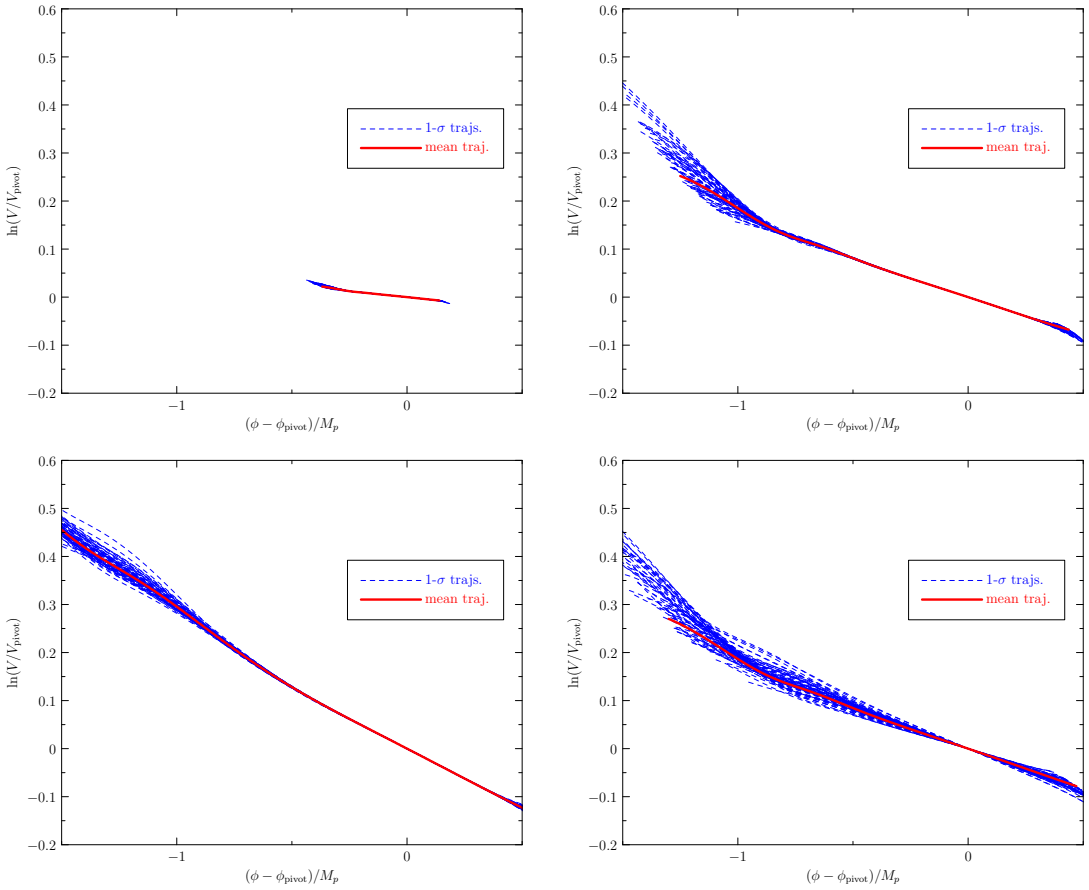

Figure 7. The reconstructed potentials with $r = 0.02$, $r = 0.2$, $r = 0.5$ and free r for top-left, top-right, bottom-left, bottom-right panels, respectively. Data: Planck + highL + BAO. BICEP2 data is added in the free r case.

of inflation ($\epsilon = 1$). The scalar and tensor power spectrum can be solved using the following equation:

$$\ddot{\mathcal{A}} + f(t)\dot{\mathcal{A}} + \frac{k^2}{a^2}\mathcal{A} - \frac{e^{-2\int^t f(t)dt}}{\mathcal{A}^3} = 0, \tag{4.6}$$

where for scalar $f(t) = 3H - 2\frac{\dot{H}}{H} + 2\frac{\ddot{\phi}}{\dot{\phi}}$ for scalar and $f(t) = 3H$ for tensor. The initial time is chosen such that $aH \ll k$. The initial asymptotic condition (for $k \gg aH$) is $\mathcal{A} \to \frac{kH}{2\pi a\dot{\phi}}$ for scalar and $\mathcal{A} \to \frac{\sqrt{2}k}{\pi a M_p}$ for tensor. Initial $\dot{\mathcal{A}}$ and the integral constant in $\int^t f(t)dt$ in eq. (4.6) are fixed by using the initial asymtotic condition. The final time is chosen such that $aH \gg k$, when $\mathcal{A}$ converges to a constant. The power spectrum $\Delta^2_{S,T}(k)$ is the square of the converged $\mathcal{A}$.

Acknowledgements

References

[1] D. J. Fixsen et al., *The cosmic microwave background spectrum from the full cobe/firas data set*, *Astrophys. J.* **473** (1996) 576, [astro-ph/9605054].

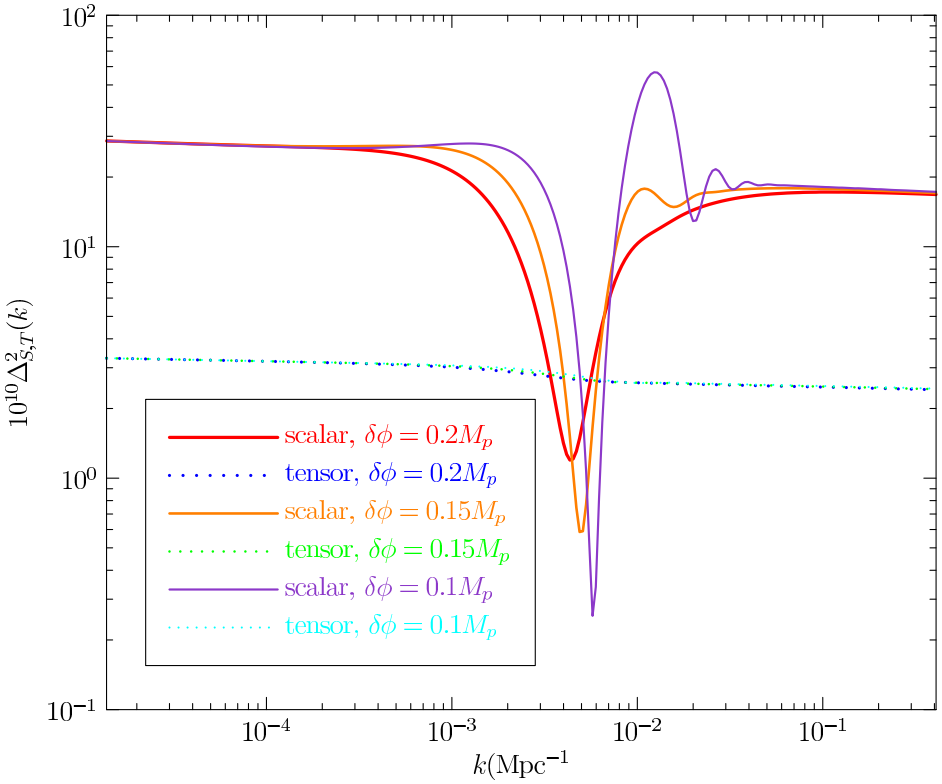

Figure 8. The primordial scalar and tensor power spectra for single-field inflation model defined in eq. (4.5). The parameters are $m = 5.7 \times 10^{-6} M_p$, $\mu = 0.1$.

[2] **Boomerang** Collaboration, C. B. Netterfield et al., *A measurement by BOOMERANG of multiple peaks in the angular power spectrum of the cosmic microwave background*, *Astrophys. J.* **571** (2002) 604–614, [astro-ph/0104460].

[3] T. Montroy, P. A. R. Ade, A. Balbi, J. J. Bock, J. R. Bond, J. Borrill, A. Boscaleri, P. Cabella, C. R. Contaldi, B. P. Crill, P. de Bernardis, G. De Gasperis, A. de Oliveira-Costa, G. De Troia, G. di Stefano, K. Ganga, E. Hivon, V. V. Hristov, A. Iacoangeli, A. H. Jaffe, T. S. Kisner, W. C. Jones, A. E. Lange, S. Masi, P. D. Mauskopf, C. MacTavish, A. Melchiorri, F. Nati, P. Natoli, C. B. Netterfield, E. Pascale, F. Piacentini, D. Pogosyan, G. Polenta, S. Prunet, S. Ricciardi, G. Romeo, J. E. Ruhl, E. Torbet, M. Tegmark, and N. Vittorio, *Measuring CMB polarization with B OOMERANG*, New A Rev. **47** (Dec., 2003) 1057–1065, [astro-ph/0305593].

[4] J. L. Sievers, R. A. Hlozek, M. R. Nolta, V. Acquaviva, G. E. Addison, P. A. R. Ade, P. Aguirre, M. Amiri, J. W. Appel, L. F. Barrientos, E. S. Battistelli, N. Battaglia, J. R. Bond, B. Brown, B. Burger, E. Calabrese, J. Chervenak, D. Crichton, S. Das, M. J. Devlin, S. R. Dicker, W. Bertrand Doriese, J. Dunkley, R. Dünner, T. Essinger-Hileman, D. Faber, R. P. Fisher, J. W. Fowler, P. Gallardo, M. S. Gordon, M. B. Gralla, A. Hajian, M. Halpern, M. Hasselfield, C. Hernández-Monteagudo, J. C. Hill, G. C. Hilton, M. Hilton, A. D. Hincks, D. Holtz, K. M. Huffenberger, D. H. Hughes, J. P. Hughes, L. Infante, K. D. Irwin, D. R. Jacobson, B. Johnstone, J. Baptiste Juin, M. Kaul, J. Klein, A. Kosowsky, J. M. Lau, M. Limon, Y.-T. Lin, T. Louis, R. H. Lupton, T. A. Marriage, D. Marsden, K. Martocci, P. Mauskopf, M. McLaren, F. Menanteau, K. Moodley, H. Moseley, C. B. Netterfield, M. D. Niemack, L. A. Page, W. A. Page, L. Parker, B. Partridge, R. Plimpton, H. Quintana, E. D. Reese, B. Reid, F. Rojas, N. Sehgal, B. D. Sherwin, B. L. Schmitt, D. N. Spergel, S. T. Staggs,

O. Stryzak, D. S. Swetz, E. R. Switzer, R. Thornton, H. Trac, C. Tucker, M. Uehara, K. Visnjic, R. Warne, G. Wilson, E. Wollack, Y. Zhao, and C. Zunckel, *The Atacama Cosmology Telescope: cosmological parameters from three seasons of data*, J. Cosmology Astropart. Phys. **10** (Oct., 2013) 60, [arXiv:1301.0824].

[5] S. Das, T. Louis, M. R. Nolta, G. E. Addison, E. S. Battistelli, J. R. Bond, E. Calabrese, D. Crichton, M. J. Devlin, S. Dicker, J. Dunkley, R. Dünner, J. W. Fowler, M. Gralla, A. Hajian, M. Halpern, M. Hasselfield, M. Hilton, A. D. Hincks, R. Hlozek, K. M. Huffenberger, J. P. Hughes, K. D. Irwin, A. Kosowsky, R. H. Lupton, T. A. Marriage, D. Marsden, F. Menanteau, K. Moodley, M. D. Niemack, L. A. Page, B. Partridge, E. D. Reese, B. L. Schmitt, N. Sehgal, B. D. Sherwin, J. L. Sievers, D. N. Spergel, S. T. Staggs, D. S. Swetz, E. R. Switzer, R. Thornton, H. Trac, and E. Wollack, *The Atacama Cosmology Telescope: temperature and gravitational lensing power spectrum measurements from three seasons of data*, J. Cosmology Astropart. Phys. **4** (Apr., 2014) 14, [arXiv:1301.1037].

[6] K. T. Story, C. L. Reichardt, Z. Hou, R. Keisler, K. A. Aird, B. A. Benson, L. E. Bleem, J. E. Carlstrom, C. L. Chang, H.-M. Cho, T. M. Crawford, A. T. Crites, T. de Haan, M. A. Dobbs, J. Dudley, B. Follin, E. M. George, N. W. Halverson, G. P. Holder, W. L. Holzapfel, S. Hoover, J. D. Hrubes, M. Joy, L. Knox, A. T. Lee, E. M. Leitch, M. Lueker, D. Luong-Van, J. J. McMahon, J. Mehl, S. S. Meyer, M. Millea, J. J. Mohr, T. E. Montroy, S. Padin, T. Plagge, C. Pryke, J. E. Ruhl, J. T. Sayre, K. K. Schaffer, L. Shaw, E. Shirokoff, H. G. Spieler, Z. Staniszewski, A. A. Stark, A. van Engelen, K. Vanderlinde, J. D. Vieira, R. Williamson, and O. Zahn, *A Measurement of the Cosmic Microwave Background Damping Tail from the 2500-Square-Degree SPT-SZ Survey*, ApJ **779** (Dec., 2013) 86, [arXiv:1210.7231].

[7] Z. Hou, C. L. Reichardt, K. T. Story, B. Follin, R. Keisler, K. A. Aird, B. A. Benson, L. E. Bleem, J. E. Carlstrom, C. L. Chang, H.-M. Cho, T. M. Crawford, A. T. Crites, T. de Haan, R. de Putter, M. A. Dobbs, S. Dodelson, J. Dudley, E. M. George, N. W. Halverson, G. P. Holder, W. L. Holzapfel, S. Hoover, J. D. Hrubes, M. Joy, L. Knox, A. T. Lee, E. M. Leitch, M. Lueker, D. Luong-Van, J. J. McMahon, J. Mehl, S. S. Meyer, M. Millea, J. J. Mohr, T. E. Montroy, S. Padin, T. Plagge, C. Pryke, J. E. Ruhl, J. T. Sayre, K. K. Schaffer, L. Shaw, E. Shirokoff, H. G. Spieler, Z. Staniszewski, A. A. Stark, A. van Engelen, K. Vanderlinde, J. D. Vieira, R. Williamson, and O. Zahn, *Constraints on Cosmology from the Cosmic Microwave Background Power Spectrum of the 2500 deg^2 SPT-SZ Survey*, ApJ **782** (Feb., 2014) 74, [arXiv:1212.6267].

[8] BICEP2 Collaboration, P. A. R. Ade, R. W. Aikin, D. Barkats, S. J. Benton, C. A. Bischoff, J. J. Bock, J. A. Brevik, I. Buder, E. Bullock, C. D. Dowell, L. Duband, J. P. Filippini, S. Fliescher, S. R. Golwala, M. Halpern, M. Hasselfield, S. R. Hildebrandt, G. C. Hilton, V. V. Hristov, K. D. Irwin, K. S. Karkare, J. P. Kaufman, B. G. Keating, S. A. Kernasovskiy, J. M. Kovac, C. L. Kuo, E. M. Leitch, M. Lueker, P. Mason, C. B. Netterfield, H. T. Nguyen, R. O'Brient, R. W. Ogburn, IV, A. Orlando, C. Pryke, C. D. Reintsema, S. Richter, R. Schwarz, C. D. Sheehy, Z. K. Staniszewski, R. V. Sudiwala, G. P. Teply, J. E. Tolan, A. D. Turner, A. G. Vieregg, C. L. Wong, and K. W. Yoon, *BICEP2 I: Detection Of B-mode Polarization at Degree Angular Scales*, *ArXiv e-prints* (Mar., 2014) [arXiv:1403.3985].

[9] C. L. Bennett, D. Larson, J. L. Weiland, N. Jarosik, G. Hinshaw, N. Odegard, K. M. Smith, R. S. Hill, B. Gold, M. Halpern, E. Komatsu, M. R. Nolta, L. Page, D. N. Spergel, E. Wollack, J. Dunkley, A. Kogut, M. Limon, S. S. Meyer, G. S. Tucker, and E. L. Wright, *Nine-year Wilkinson Microwave Anisotropy Probe (WMAP) Observations: Final Maps and Results*, ApJS **208** (Oct., 2013) 20, [arXiv:1212.5225].

[10] G. Hinshaw, D. Larson, E. Komatsu, D. N. Spergel, C. L. Bennett, J. Dunkley, M. R. Nolta, M. Halpern, R. S. Hill, N. Odegard, L. Page, K. M. Smith, J. L. Weiland, B. Gold, N. Jarosik, A. Kogut, M. Limon, S. S. Meyer, G. S. Tucker, E. Wollack, and E. L. Wright, *Nine-year Wilkinson Microwave Anisotropy Probe (WMAP) Observations: Cosmological Parameter Results*, ApJS **208** (Oct., 2013) 19, [arXiv:1212.5226].

[11] Planck Collaboration, P. A. R. Ade, N. Aghanim, C. Armitage-Caplan, M. Arnaud, M. Ashdown, F. Atrio-Barandela, J. Aumont, C. Baccigalupi, A. J. Banday, and et al., *Planck 2013 results. I. Overview of products and scientific results*, *ArXiv e-prints* (Mar., 2013) [arXiv:1303.5062].

[12] Planck collaboration, P. A. R. Ade, N. Aghanim, C. Armitage-Caplan, M. Arnaud, M. Ashdown, F. Atrio-Barandela, J. Aumont, C. Baccigalupi, A. J. Banday, and et al., *Planck 2013 results. XV. CMB power spectra and likelihood*, *ArXiv e-prints* (Mar., 2013) [arXiv:1303.5075].

[13] Planck Collaboration, P. A. R. Ade, N. Aghanim, C. Armitage-Caplan, M. Arnaud, M. Ashdown, F. Atrio-Barandela, J. Aumont, C. Baccigalupi, A. J. Banday, and et al., *Planck 2013 results. XVI. Cosmological parameters*, *ArXiv e-prints* (Mar., 2013) [arXiv:1303.5076].

[14] S. Kachru, R. Kallosh, A. Linde, and S. P. Trivedi, *De sitter vacua in string theory*, *Phys. Rev.* **D68** (2003) 046005, [hep-th/0301240].

[15] J. J. Blanco-Pillado, C. P. Burgess, J. M. Cline, C. Escoda, M. Gomez-Reino, R. Kallosh, A. Linde, and F. Quevedo, *Racetrack inflation*, *JHEP* **11** (2004) 063, [hep-th/0406230].

[16] J. J. Blanco-Pillado, C. P. Burgess, J. M. Cline, C. Escoda, M. Gomez-Reino, R. Kallosh, A. Linde, and F. Quevedo, *Inflating in a better racetrack*, *JHEP* **09** (2006) 002, [hep-th/0603129].

[17] S. Kachru, R. Kallosh, A. Linde, J. Maldacena, L. McAllister, and S. P. Trivedi, *Towards inflation in string theory*, *JCAP* **0310** (2003) 013, [hep-th/0308055].

[18] J. P. Conlon and F. Quevedo, *Kaehler moduli inflation*, *JHEP* **01** (2006) 146, [hep-th/0509012].

[19] S. B. Giddings, S. Kachru, and J. Polchinski, *Hierarchies from fluxes in string compactifications*, *Phys. Rev.* **D66** (2002) 106006, [hep-th/0105097].

[20] E. Silverstein and A. Westphal, *Monodromy in the CMB: Gravity Waves and String Inflation*, *Phys. Rev.* **D78** (2008) 106003, [arXiv:0803.3085].

[21] A. D. Linde and V. F. Mukhanov, *Nongaussian isocurvature perturbations from inflation*, *Phys. Rev.* **D56** (1997) 535–539, [astro-ph/9610219].

[22] A. A. Starobinsky, *Beyond the simplest inflationary cosmological models.*, *Gravitation and Cosmology* **4** (1998) 88–99, [astro-ph/].

[23] D. H. Lyth and D. Wands, *The CDM isocurvature perturbation in the curvaton scenario*, *Phys. Rev.* **D68** (2003) 103516, [astro-ph/0306500].

[24] N. Barnaby and Z. Huang, *Particle production during inflation: Observational constraints and signatures*, *Phys. Rev. D* **80** (Dec, 2009) 126018.

[25] J. R. Bond, A. V. Frolov, Z. Huang, and L. Kofman, *Non-Gaussian Curvature Spikes from Chaotic Billiards in Inflation Preheating*, *Physical Review Letters* **103** (Aug., 2009) 071301–+, [arXiv:0903.3407].

[26] A. Kosowsky and M. S. Turner, *CBR anisotropy and the running of the scalar spectral index*, Phys. Rev. D **52** (Aug., 1995) 1739, [astro-ph/9504071].

[27] A. Lewis and S. Bridle, *Cosmological parameters from cmb and other data: a monte- carlo approach*, *Phys. Rev.* **D66** (2002) 103511, [astro-ph/0205436].

[28] C. P. Ahn, R. Alexandroff, C. Allende Prieto, S. F. Anderson, T. Anderton, B. H. Andrews, É. Aubourg, S. Bailey, E. Balbinot, R. Barnes, and et al., *The Ninth Data Release of the Sloan Digital Sky Survey: First Spectroscopic Data from the SDSS-III Baryon Oscillation Spectroscopic Survey*, ApJS **203** (Dec., 2012) 21, [arXiv:1207.7137].

[29] D. H. Jones, W. Saunders, M. Colless, M. A. Read, Q. A. Parker, F. G. Watson, L. A. Campbell, D. Burkey, T. Mauch, L. Moore, M. Hartley, P. Cass, D. James, K. Russell, K. Fiegert, J. Dawe, J. Huchra, T. Jarrett, O. Lahav, J. Lucey, G. A. Mamon, D. Proust, E. M. Sadler, and K.-i. Wakamatsu, *The 6dF Galaxy Survey: samples, observational techniques and the first data release*, MNRAS **355** (Dec., 2004) 747–763, [astro-ph/0403501].

[30] D. H. Jones, M. A. Read, W. Saunders, M. Colless, T. Jarrett, Q. A. Parker, A. P. Fairall, T. Mauch, E. M. Sadler, F. G. Watson, D. Burton, L. A. Campbell, P. Cass, S. M. Croom, J. Dawe, K. Fiegert, L. Frankcombe, M. Hartley, J. Huchra, D. James, E. Kirby, O. Lahav, J. Lucey, G. A. Mamon, L. Moore, B. A. Peterson, S. Prior, D. Proust, K. Russell, V. Safouris, K.-I. Wakamatsu, E. Westra, and M. Williams, *The 6dF Galaxy Survey: final redshift release (DR3) and southern large-scale structures*, MNRAS **399** (Oct., 2009) 683–698, [arXiv:0903.5451].